LHC data on inelastic diffraction and uncertainties in the predictions for longitudinal extensive air shower development

S. Ostapchenko[*]

D. V. Skobeltsyn Institute of Nuclear Physics, Moscow State University, 119991 Moscow, Russia

The present status of experimental studies of inelastic diffraction at the Large Hadron Collider is analyzed. The impact of the current uncertainties concerning the diffraction rate on the predicted extensive air shower development is investigated. A relation to studies of the primary composition of ultrahigh energy cosmic rays is illustrated by comparing numerical simulation results to the data of the Telescope Array experiment on the distributions of the shower maximum position.

PACS numbers: 13.85.-t, 12.38.Lg

I. INTRODUCTION

Among the most outstanding problems in the high energy cosmic ray (CR) field is the determination of the composition of ultrahigh energy cosmic rays (UHECRs). The corresponding experimental studies are based on the so-called extensive air shower (EAS) technique [1]: the properties of primary cosmic ray particles (protons and nuclei) are reconstructed from measured characteristics of nuclear-electromagnetic cascades induced by them in the atmosphere. Respectively, the obtained results depend strongly on the correctness of the Monte Carlo (MC) procedures used for numerical simulations of air showers, notably, on the models of hadronic interactions, employed in such simulation programs. This brings an additional source of uncertainty for the experimental results—as such models are largely phenomenological ones and have to be extrapolated from accelerator energies, where they are calibrated, to the much higher UHECR energies [2].

In this respect, experimental data on proton-proton interactions, obtained at the Large Hadron Collider (LHC) at the highest collision energies thus far, prove to be invaluable for improving EAS simulation procedures, reducing thereby the above-discussed uncertainty in CR studies. Importantly, a comparison of the predictions of hadronic MC generators with LHC data revealed that hadronic interaction models used in the CR field provide adequate enough description of the main features of proton-proton interactions [3]. Moreover, a number of model updates emerged recently [4–6], which included new fine-tunings of model parameters, based on LHC data, as well as improvements in the underlying theoretical framework. Nevertheless, there remain considerable differences between the model predictions for basic EAS characteristics, which constitute a serious obstacle for precise studies of the UHECR composition [7].

Presently, mass composition of high energy cosmic rays is studied by two different techniques [1]: (i) via

measurements of lateral densities of all charged particles and of muons only by ground-based detectors; (ii) via studies of the longitudinal shower development with fluorescence detectors. While both methods can generally be powerful enough for determining the UHECR composition, the progress of the ground-based studies is presently hampered by the strong contradiction between the data of the Pierre Auger Observatory for EAS muon content at primary CR energies $E_0 > 3 \times 10^{18}$ eV and the respective predictions of the shower simulation procedures [8]. The reported large (factor 1.3–1.6) discrepancy between the Pierre Auger Observatory data and the simulation results is especially surprising in view of the above-mentioned calibration of hadronic interaction models to LHC data. Moreover, no such contradiction has been observed by the KASCADE-Grande experiment at slightly lower energies ($E_0 < 10^{18}$ eV) [9]. In view of this confusing situation, we shall restrict our analysis to the observables related to the longitudinal EAS development, namely, to the position of the shower maximum $X_{\max}$ (the depth in the atmosphere where a maximal number of ionizing particles is observed) and its distribution.

Remarkably, the shower maximum position for proton-induced EAS depends mostly on characteristics of the interaction of the primary cosmic ray particle with air nuclei, notably on the respective inelastic cross section $\sigma_{p\text{-air}}^{\mathrm{inel}}$. Hence, recent precise measurements (with percent level accuracy) of the total, elastic, and inelastic proton-proton cross sections at $\sqrt{s} = 7$ and 8 TeV by the TOTEM experiment [10–14] provide extremely important constraints for the respective model predictions—as $\sigma_{p\text{-air}}^{\mathrm{inel}}$ can thus be calculated in the framework of the Glauber-Gribov approach [15,16].

Unfortunately, additional uncertainties arise from the treatment of inelastic diffraction in hadronic interaction models, which impacts model predictions for $X_{\max}$ in two ways. First, inelastic diffraction is intimately related to the inelastic screening effect for the calculated cross sections of hadron-proton and hadron-nucleus interactions [16]: a higher

[*]sergei@tf.phys.ntnu.no

TABLE I. $\sigma_{pp}^{\mathrm{SD}}$ (mb) at $\sqrt{s} = 7$ TeV for different ranges of mass M_X of diffractive states produced.

M_X range	< 3.4 GeV	3.4–1100 GeV	3.4–7 GeV	7–350 GeV	350–1100 GeV
TOTEM [12,22]	2.62 ± 2.17	6.5 ± 1.3	$\simeq 1.8$	$\simeq 3.3$	$\simeq 1.4$
QGSJET-II-04	3.9	7.2	1.9	3.9	1.5
Option SD+	3.2	8.2	1.8	4.7	1.7
Option SD−	2.6	7.2	1.6	3.9	1.7

rate of diffraction dissociation is accompanied by stronger screening effects which give rise to a smaller hadron-nucleus cross section predicted (e.g., [17]). Secondly, the rate of inelastic diffraction largely dominates model predictions for the so-called inelasticity $K_{p\text{-air}}^{\mathrm{inel}}$, the relative energy loss of the leading (most energetic) secondary nucleon in p-air collisions. For example, in the target diffraction process at very high energies the leading proton loses only a tiny fraction of its energy: $\Delta E/E_0 \simeq \exp(-\Delta y) \ll 1$, where Δy is the size of the rapidity gap between the struck proton and the most energetic secondary hadron produced in the diffractive excitation of the target nucleus.[1] Thus, enhancing target diffraction is equivalent to effectively reducing the total inelastic cross section $\sigma_{p\text{-air}}^{\mathrm{inel}}$. As both above-discussed effects work in the same direction, one has a simple "rule of thumb": higher diffraction rate corresponds to a slower EAS development (deeper shower maximum) and vice versa.

In the following, we are going to investigate the impact of the present experimental uncertainties concerning the rate of the inelastic diffraction in hadronic collisions on model predictions for the longitudinal EAS development and on the related studies of the UHECR composition. Our analysis will be based on the QGSJET-II-04 model [4], which is characterized by a microscopic treatment of nonlinear interaction effects in hadronic collisions and thus, has a much higher predictive power for various interaction characteristics, notably for diffractive cross sections, compared to other MC generators.

The paper is organized as follows. In Sec. II, we review recent LHC results on inelastic diffraction and illustrate certain tensions between the data of different experiments by comparing them to predictions of the QGSJET-II-04 model. Additionally, we perform two additional tunes of the model parameters, designed to fit better different sets of measurements. The predictions of these two alternative model versions for the average X_{max} and its fluctuations are compared in Sec. III and the respective differences are regarded as the corresponding model uncertainty. Further, we illustrate the potential impact of this uncertainty on UHECR composition studies by applying the alternative model versions to fitting X_{max} distributions measured by the Telescope Array experiment. We conclude in Sec. IV.

II. LHC RESULTS ON INELASTIC DIFFRACTION

Studies of the inelastic diffraction constitute an important part of the experimental program at the Large Hadron Collider, with important results obtained by the ALICE [18], ATLAS [19], CMS [20], and TOTEM [12,21,22] experiments. Unfortunately, at the present stage there exist certain tensions between TOTEM measurements of diffractive cross sections and the respective CMS and ATLAS results, as already discussed in Refs. [23,24].

To get a deeper insight into the problem, we start by comparing the results of the TOTEM and CMS experiments for the cross section of single diffraction $\sigma_{pp}^{\mathrm{SD}}$, for different ranges of mass M_X of diffractive states produced, with the predictions of the QGSJET-II-04 model: Tables I, II, and Fig. 1 (left panel). It is easy to see that the M_X dependencies observed by the two experiments qualitatively agree with each other and with the model predictions. However, the absolute rates of the inelastic diffraction measured by TOTEM and CMS are noticeably different: while the results of QGSJET-II-04 agree with TOTEM values within the reported experimental uncertainties, the model predictions appear to be in variance with the CMS measurements, lacking some 30% of $\sigma_{pp}^{\mathrm{SD}}$ observed by CMS. The discussed contradiction is surprising considering the fact that the kinematic range studied by CMS ($12 < M_X < 394$ GeV) is fully covered by TOTEM ($3.4 < M_X < 1100$ GeV). In principle, as the CMS analysis is based on the rapidity gap technique, its results depend noticeably on model-dependent corrections. A relevant example is the subtraction of the contribution of double diffraction, when one of the diffractively excited states is characterized by a small mass ($M_Y < 3$ GeV) and thus remains unobserved by the experimental apparatus. Such a contribution is potentially dangerous as the MC generators used in the analysis lack any specific treatment for low mass diffraction, notably for the diffractive production of low mass resonance states (e.g., N^*), as stressed previously in [25]. As an illustration, we plot in Fig. 1 (left panel) the results for the sum of $\sigma_{pp \to Xp}^{\mathrm{SD}}$ and $\sigma_{pp \to XY}^{\mathrm{DD}}(M_Y < 3$ GeV) for the M_X range studied by CMS (blue dashed line).

TABLE II. $\sigma_{pp}^{\mathrm{SD}}$ (mb) at $\sqrt{s} = 7$ TeV for $12 < M_X < 394$ GeV.

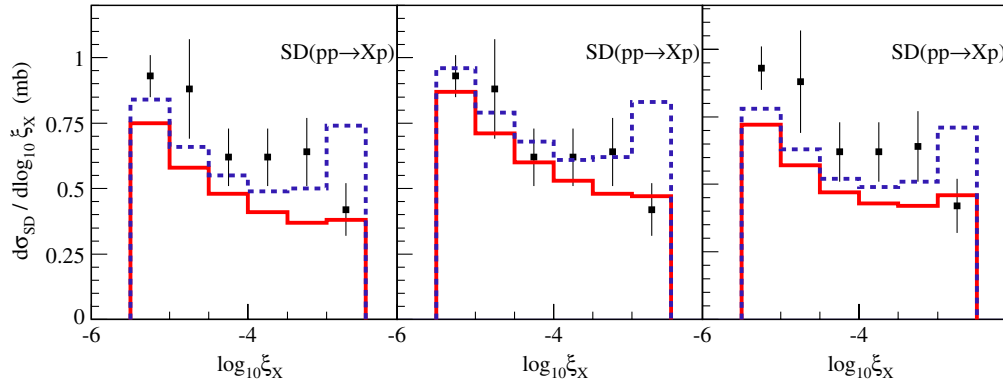| [20]	QGSJET-II-04	Option SD+	Option SD−
4.3 ± 0.6	3.0	3.7	3.1

---

[1]Typically, $\Delta y \gtrsim \ln \sqrt{s}$.

FIG. 1 (color online).   Calculated $\xi_X \equiv M_X^2/s$ dependence of $\sigma_{pp \to Xp}^{SD}$ at $\sqrt{s} = 7$ TeV (full histograms) compared to CMS data [20] (points) for QGSJET-II-04 (left), option SD+ (middle), and option SD− (right). The same dependence for $\sigma_{pp \to Xp}^{SD} + \sigma_{pp \to XY}^{DD}$ ($M_Y < 3$ GeV) is shown by dashed histograms.

However, even in that case one is unable to reach a satisfactory agreement between the model results and the CMS data.

Moreover, comparing in Fig. 2 the model predictions for the cross section for forward rapidity gap production $d\sigma_{pp}/d\Delta\eta_F$, $\Delta\eta_F$ being the forward rapidity gap size, with respective ATLAS data [19], we see the same level of disagreement (30%–40%) despite the fact that both single and double diffraction processes contribute to the studied cross sections. A potential way out of the contradiction is to assume that QGSJET-II-04 seriously underestimates the contribution of double diffraction and that the latter dominates $d\sigma_{pp}/d\Delta\eta_F$ and also contaminates noticeably σ_{pp}^{SD} measured by CMS. Comparing the prediction of the model for the cross section of high mass diffraction $\sigma_{pp \to XY}^{DD}$

($M_X, M_Y > 10$ GeV), with the rapidity gap between the two diffractive states $\Delta\eta > 3$, with the CMS data in Fig. 3 and Table III, we find indeed a rather large (∼40%) disagreement which is, however, insufficient to explain the above-discussed discrepancies (cf. the contribution of double diffraction to $d\sigma_{pp}/d\Delta\eta_F$ in Fig. 2). Moreover, the model prediction for the rate of double diffraction proves to be in good agreement with TOTEM measurements; see Table IV.

Generally, the TOTEM experiment has a good potential for reliable measurements of diffractive cross sections— thanks to the roman pot technique employed. However, at the present stage we have no choice but to regard the differences between the preliminary TOTEM results and the ones of the CMS and ATLAS experiments as the experimental uncertainty for the diffraction rates. In the
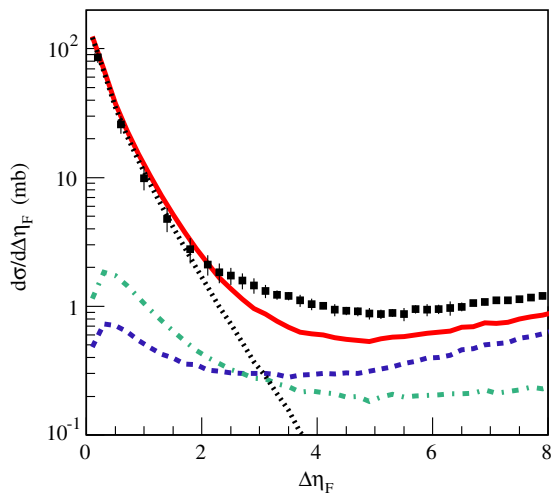

FIG. 2 (color online).   Cross section for forward rapidity gap production in pp collisions at $\sqrt{s} = 7$ TeV, calculated with QGSJET-II-04 (solid line), in comparison with ATLAS data [19] (points). Separately shown are contributions from single diffractive (dashed), double diffractive (dot-dashed), and nondiffractive (dotted) interactions.
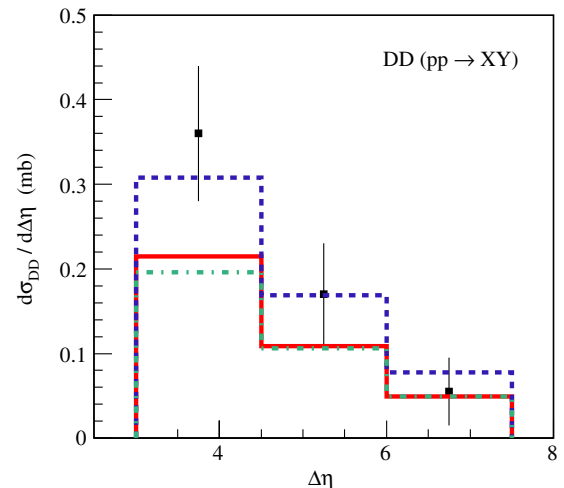

FIG. 3 (color online).   Calculated $\sigma_{pp \to XY}^{DD}$ (mb) at $\sqrt{s} = 7$ TeV as a function of the rapidity gap size $\Delta\eta = -\log(M_X^2 M_Y^2/(s \cdot m_p^2))$ (m_p being the proton mass) for $M_X, M_Y > 10$ GeV compared to CMS data [20] (points) for QGSJET-II-04 (solid), option SD+ (dashed), and option SD− (dot-dashed).

TABLE III. $\sigma^{DD}_{pp\to XY}$ (mb) at $\sqrt{s} = 7$ TeV for $M_X, M_Y > 10$ GeV and $\Delta\eta > 3$.

CMS [20]	QGSJET-II-04	Option SD+	Option SD−
$0.93 \pm 0.01^{+0.26}_{-0.22}$	0.57	0.85	0.54

TABLE IV. σ^{DD}_{pp} (μb) at $\sqrt{s} = 7$ TeV for the minimum pseudorapidity of produced hadrons $4.7 < |\eta_{min}| < 6.5$.

TOTEM [21]	QGSJET-II-04	Option SD+	Option SD−
116 ± 25	134	152	102

next section, we are going to investigate the impact of this uncertainty on the model predictions for X_{max} and for related studies of UHECR composition. To this end, we create two additional versions of the model, with alternative tunes of its parameters. In one case, referred to below as "option SD+," we enhance the contribution of high mass diffraction[2] in order to reach a reasonable agreement with ATLAS and CMS—see Figs. 1 (middle panel), 3, and 4, and also Tables II and III. At the same time, we slightly reduce the rate of low mass diffraction—in order to soften the obtained disagreement with TOTEM (Tables I and IV). Alternatively, we choose to fit more closely the TOTEM result for the low mass diffraction cross section [12] by seriously reducing the respective contribution (by as much as 30%), while keeping more or less the same rate for high mass diffraction ("option SD−"). The respective results are compared to the TOTEM, CMS, and ATLAS data in Tables I–IV and Figs. 1 (right panel), 3, and 4. In addition, the option SD+ is characterized by a slightly slower energy rise of the total and inelastic cross sections, while the opposite is true for the option SD−, both within the experimental uncertainties (Fig. 5). For both versions, model parameters are tuned in such a way that particle production in the central rapidity range remains similar to the original QGSJET-II-04, as illustrated in Fig. 6.

III. IMPACT ON X_{max} PREDICTIONS AND ON UHECR COMPOSITION STUDIES

Now we apply both the original QGSJET-II-04 and the two alternative model versions to air shower simulations, using the CONEX program [30]. The obtained primary energy dependencies of the predicted average X_{max} and of the corresponding shower maximum distribution width RMS(X_{max}) for the three models considered are presented

[2]Technically, a higher rate for high mass diffraction is obtained by increasing the value of the triple-Pomeron coupling in the model, which thus impacts both single and double diffraction processes [4,26]. In turn, the rate of low mass diffraction is governed by the structure of Good-Walker diffractive eigenstates, notably, by their relative interaction strengths [17].
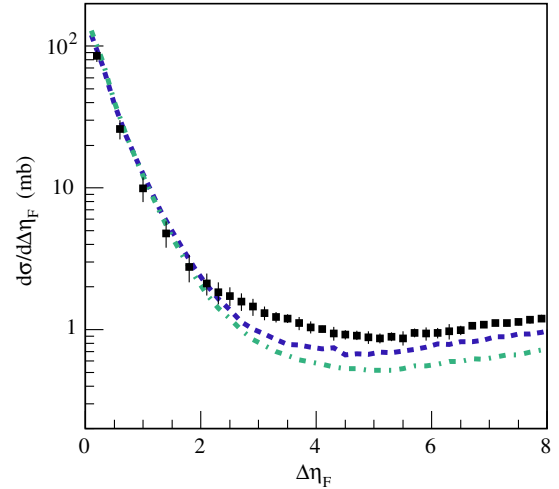

FIG. 4 (color online). Cross section for forward rapidity gap production in pp collisions at $\sqrt{s} = 7$ TeV, calculated with the options SD+ (dashed) and SD− (dot-dashed), compared to ATLAS data [19] (points).

in Fig. 7. The plots demonstrate how the present experimental uncertainties concerning the rate of inelastic diffraction project themselves on the predicted EAS characteristics. While the respective uncertainties for RMS(X_{max}) prove to be negligibly small (less than 3 g/cm^2), those for the average shower maximum position appear to be quite sizable: X_{max} predictions for the two alternative model versions (options SD+ and SD−) differ from each other by some 10 g/cm^2. While being already smaller than typical experimental inaccuracies of X_{max} measurements (15–20 g/cm^2), these model uncertainties may noticeably degrade the accuracy of UHECR composition studies.
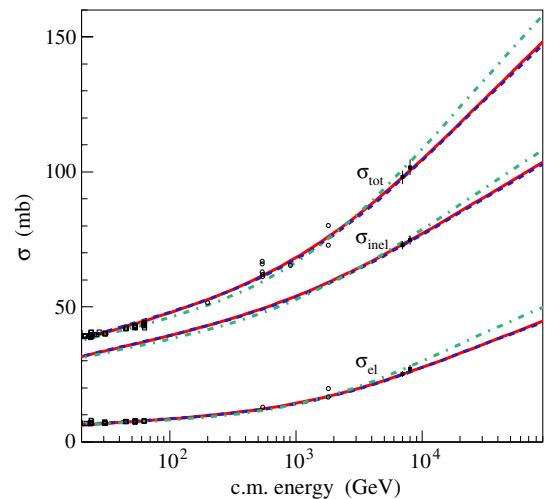

FIG. 5 (color online). Energy dependence of total, inelastic, and elastic pp cross sections as calculated using the default QGSJET-II-04 model (solid), option SD+ (dashed), and option SD− (dot-dashed). Experimental data are from [13,14,27].
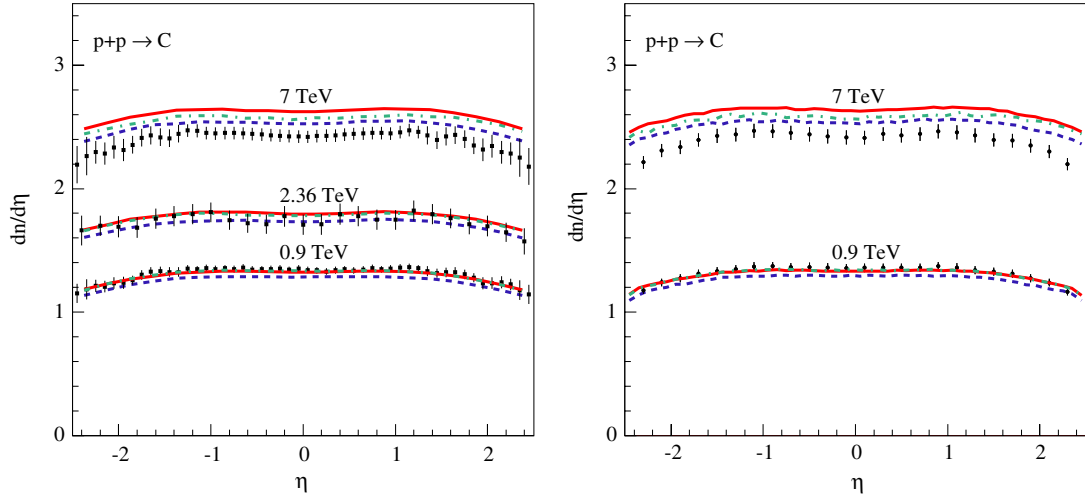
FIG. 6 (color online). Pseudorapidity density of charged hadrons of transverse momentum $p_t > 0.5$ GeV produced in pp collisions at $\sqrt{s} = 0.9, 2.36$, and 7 TeV (as indicated in the plots) as calculated using the default QGSJET-II-04 model (solid), option SD+ (dashed), and option SD− (dot-dashed) compared to experimental data from ATLAS [28] (squares) and CMS [29] (circles).
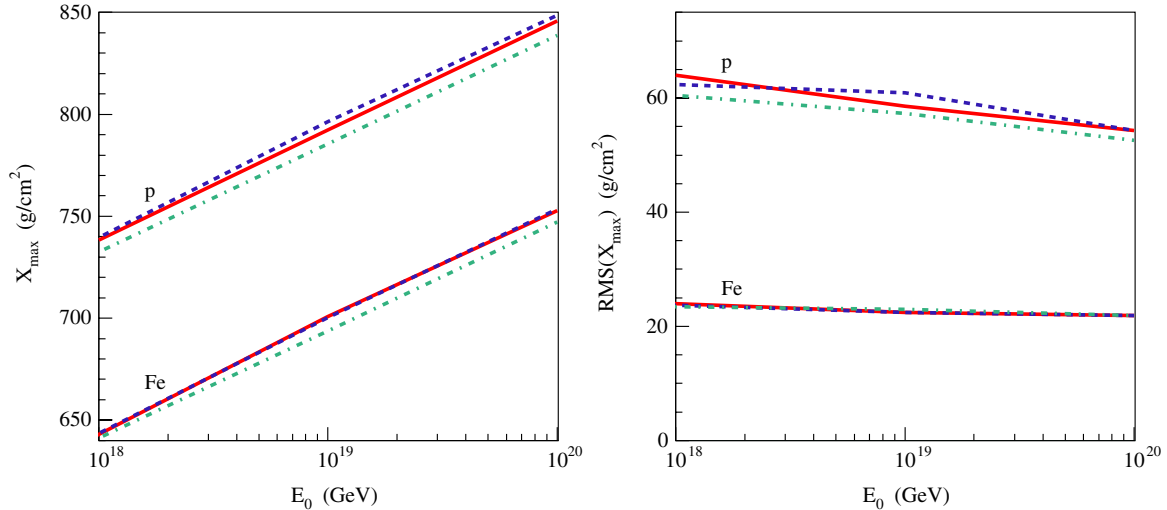

FIG. 7 (color online). Average X_{max} (left) and RMS(X_{max}) (right) for the default QGSJET-II-04 model (solid), option SD+ (dashed), and option SD− (dot-dashed).

To illustrate the latter point, we apply the above-described model versions to a simplified analysis of the cosmic ray composition in the very high energy range, using the data of the Telescope Array (TA) experiment [31]. In principle, as demonstrated already in Ref. [32], the width of X_{max} distributions RMS(X_{max}) could be a very convenient tool for CR composition studies: the quantity is practically independent of any other details of interaction models used for EAS simulations, except the predicted total inelastic cross section and the inelastic diffraction rate. However, experimental determination of RMS(X_{max}) is somewhat challenging due to its sensitivity to data quality cuts employed in a particular analysis and to other details of experimental procedures. Therefore, correcting for such

effects, inherent for a particular experiment, is a nontrivial problem. Hence, we apply here a more standard method, trying to deduce the primary composition from fitting the measured X_{max} distributions by simulated ones, for different mixtures of primary CR particles.

TABLE V. Parameters for the composition fit [Eq. (1)] based on Telescope Array X_{max} data.

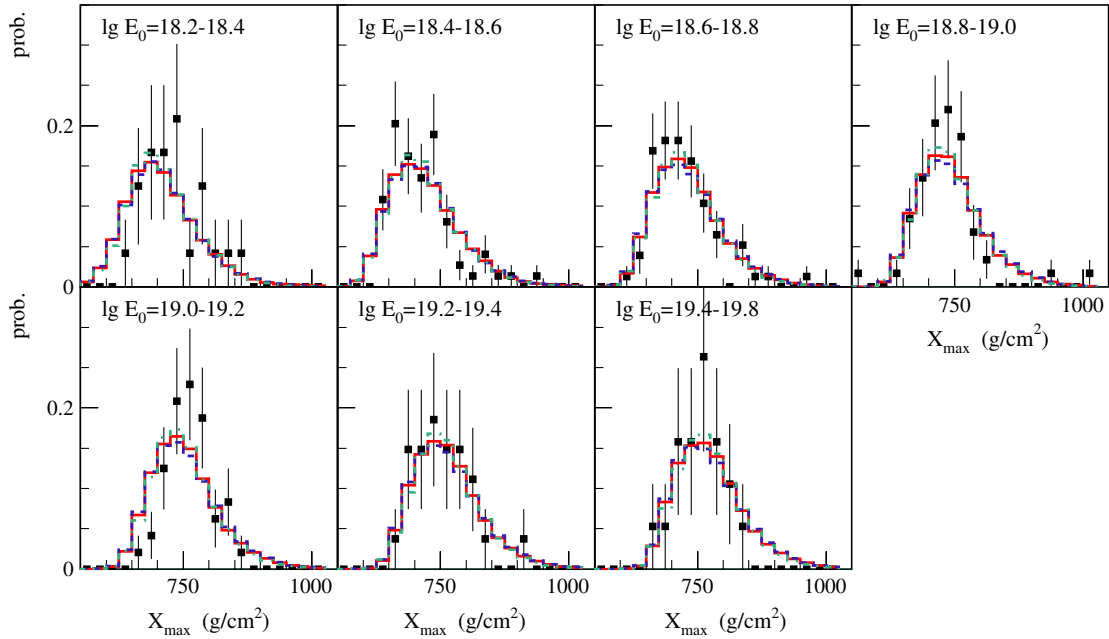|	$d_p(1)$	$d_p(100)$	χ^2/d.o.f.
QGSJET-II-04	0.79	0.77	35.6/33
Option SD+	0.77	0.75	41.4/33
Option SD−	0.84	0.85	31.8/33

FIG. 8 (color online). X_{max} distributions measured by the Telescope Array experiment [31] compared to calculations with the default QGSJET-II-04 model (solid), option SD+ (dashed), and option SD− (dot-dashed) for the fitted primary compositions from Table V.

As the measured X_{max} distributions are influenced by experimental measurement and reconstruction procedures, the consistency requires the output of EAS simulation procedures to be processed through the same analysis and reconstruction chains as the respective experimental data. In this work, we choose an alternative way: we mimic the above-discussed effects by applying a systematic shift ΔX_{max} and an additional Gaussian smearing $\Delta\sigma$ to X_{max} distributions obtained from EAS simulations, as described in more detail in the Appendix. Using this method, we fit X_{max} distributions measured by the Telescope Array experiment in a number of primary energy intervals, using a two-component mixture (p plus Fe) for the primary CR composition and assuming the relative abundances d_i ($i = p, Fe$) to depend logarithmically on the energy of the primary particle E_0:

$$d_p(E_0) = d_p(1) + [d_p(100) - d_p(1)]\lg(E_0/1\text{EeV})/2$$
$$d_{Fe}(E_0) = 1 - d_p(E_0). \tag{1}$$

Here $d_p(1)$ and $d_p(100)$ refer to proton abundances at 1 and 100 EeV, respectively.

The fitted primary abundances are presented in Table V, while the corresponding X_{max} distributions are shown in Fig. 8 in comparison to the experimental data. We attempted also to fit the data with a three-component composition mixture, adding either helium or carbon nuclei as the third primary group, but we have not obtained a significant improvement of the quality of the fits.

It is easy to see that the obtained fraction of primary iron nuclei is very sensitive to the uncertainties studied in this work, amounting to a 10% difference between the options SD+ and SD−. One may equally well fit the data with an energy-independent composition mixture [$d_p(E_0) = d_p = $ const], as illustrated in Fig. 9. Here we see how the uncertainties related to inelastic diffraction rate may influence the interpretation of experimental data: while for the model option SD− the data are consistent with an almost pure proton composition in the energy range $E_0 = 10^{18}–10^{20}$ eV, this is no longer valid for the option SD+, in which case a substantial fraction of heavy nuclei is required. These differences may have long-ranging consequences for astrophysical interpretations of UHECR data, e.g., for discriminating between models for the transition from galactic to extragalactic cosmic ray origin in the ultrahigh energy range (see [33] for a recent review).
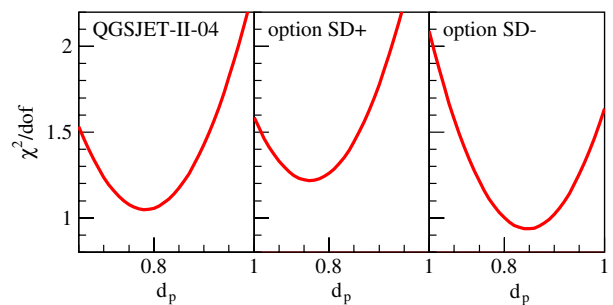

FIG. 9 (color online). Goodness of fits to the TA X_{max} distributions for an energy-independent primary composition with proton fraction d_p, using different interaction models (as indicated in the plots).

TABLE VI.   Applied Gaussian smearing width $\Delta\sigma$ (in g/cm^2) for different primary energy bins for p- and Fe-induced EAS.

lg E_0	18.2–18.4	18.4–18.6	18.6–18.8	18.8–19.0	19.0–19.2	19.2–19.4	19.4–19.6	19.6–19.8
$\Delta\sigma_p$	21	20	19	12	14	18	19	13
$\Delta\sigma_{Fe}$	28	19	18	17	19	18	17	18

IV. SUMMARY

We discussed recent LHC results on inelastic diffraction in pp collisions and demonstrated that there exists a substantial uncertainty concerning the rate of diffractive collisions. This latter projects itself on model-based calculations of the development of CR-induced extensive air showers in the atmosphere, resulting in some 10 g/cm^2 uncertainty for the predicted shower maximum position $X_{\max}$. Though being already smaller than the typical experimental precision for $X_{\max}$ measurements, this uncertainty may noticeably degrade

the accuracy of UHECR composition studies and, as demonstrated above, can even seriously bias astrophysical interpretations of cosmic ray data. Thus, further progress in experimental studies of inelastic diffraction at the Large Hadron Collider is of utmost importance for the cosmic ray field.

One may question if there exist other uncertainties which impact model predictions for the longitudinal air shower development. Unfortunately, this is indeed the case: predicted $X_{\max}$ depends noticeably on the multiplicity of
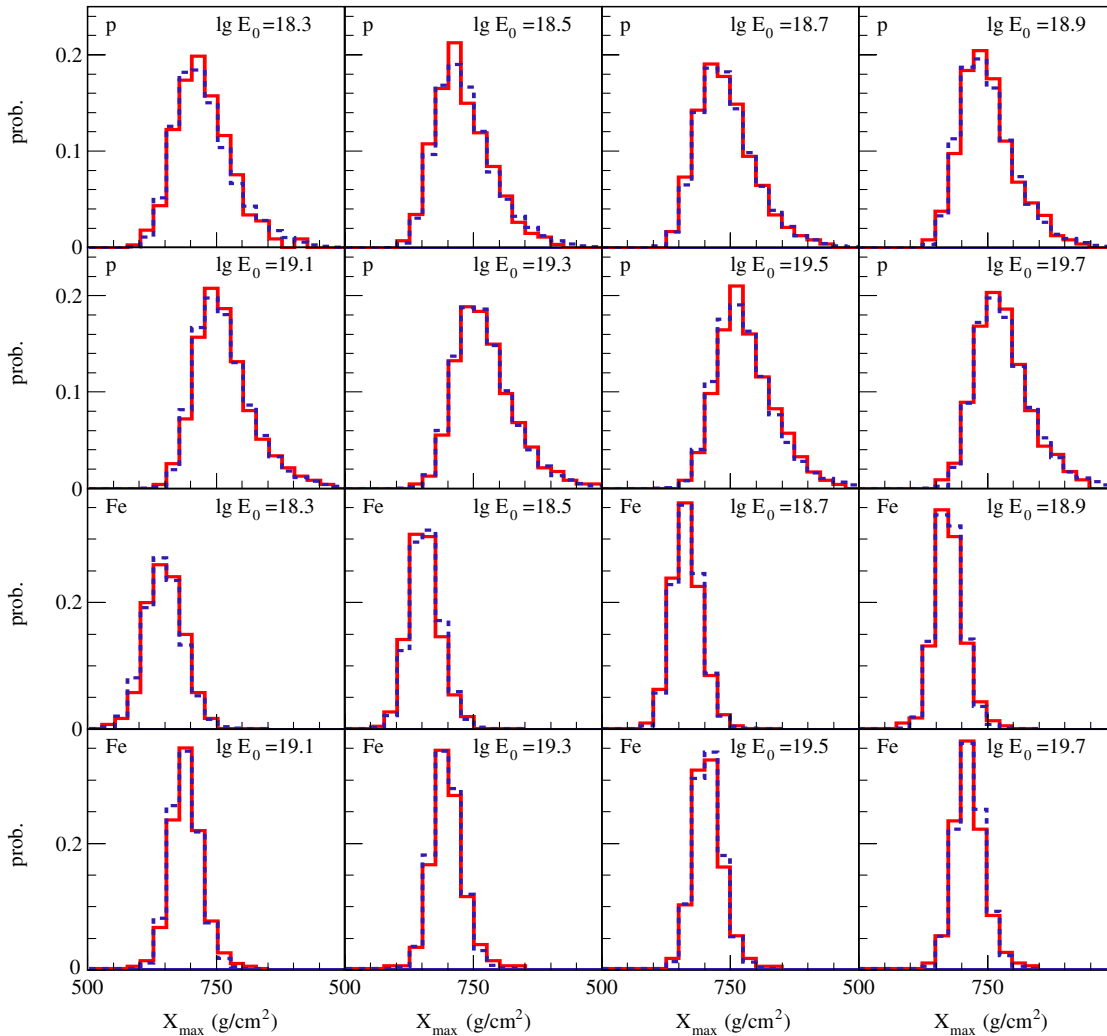

FIG. 10 (color online). $X_{\max}$ distributions from TA analysis [31] with QGSJET-II-03 (full histograms) compared to simulation results with $X_{\max}$-shift $\Delta X_{\max}$ and Gaussian smearing $\Delta\sigma$ applied (dashed histograms).

secondary particles in proton-air interactions [34]. Present LHC data appear to be insufficient to fully remove this uncertainty due to a significant model dependence for the generalization from pp to pA collisions. In particular, it is the smaller multiplicity of proton-nitrogen collisions, predicted by the EPOS-LHC model compared to QGSJET-II-04, which is the reason for deeper X_{max} predicted by that model (by as much as 20 g/cm^2) [7]. Thus, experimental studies of collisions of protons with light nuclei (nitrogen or oxygen) at LHC could be very useful for finally settling the issue.

ACKNOWLEDGMENTS

The author is indebted to V. Berezinsky for motivating discussions which stimulated this investigation. Useful discussions with M. Kacheriess, V. Khoze, T. Pierog, and M. Unger are gratefully acknowledged.

APPENDIX

Measured distributions of the shower maximum position X_{max} are influenced by experimental quality cuts and by reconstruction procedures employed in experimental analysis. Therefore, to compare numerical simulation results to the data and to perform an analysis of the cosmic rays' composition, the output of EAS simulation procedures has to be processed through the same analysis and reconstruction chains as the respective experimental data.

In this work, we choose an alternative way: we mimic the above-discussed effects by applying a systematic shift ΔX_{max} and an additional Gaussian smearing $\Delta\sigma$ to X_{max} distributions obtained from EAS simulations. In the case of TA data, the values of ΔX_{max} and $\Delta\sigma$ are defined via a least squares minimization of the difference between the X_{max} distributions thus modified, which were obtained with the QGSJET-II-03 model [35], and the respective simulation results of the Telescope Array collaboration, based on the same interaction model, which were obtained via processing the model predictions through the complete experimental analysis and reconstruction chain [31]. Subsequently, we apply the shift and smearing parameters thus obtained to X_{max} distributions obtained both with the default QGSJET-II-04 model and with the two alternative model tunings described in the text in order to compare the model results to experimental data. As all the above-discussed models have more or less the same physics content and their predicted X_{max} distributions have similar shapes, we believe the procedure is accurate enough for the purposes of the present investigation.

In more detail, we applied uniform (energy-independent) shifts $\Delta X_{max}^{p} = -25$ g/cm^2 and $\Delta X_{max}^{Fe} = -21$ g/cm^2 in case of p-induced and Fe-induced EAS, respectively, while adjusting the Gaussian smearing width $\Delta\sigma$ individually for each primary energy bin; see Table VI. X_{max} distributions obtained this way (using QGSJET-II-03) are compared to TA simulation results in Fig. 10.

[1] M. Nagano and A. A. Watson, Rev. Mod. Phys. **72**, 689 (2000).
[2] R. Engel, D. Heck, and T. Pierog, Annu. Rev. Nucl. Part. Sci. **61**, 467 (2011).
[3] D. d'Enterria, R. Engel, T. Pierog, S. Ostapchenko, and K. Werner, Astropart. Phys. **35**, 98 (2011).
[4] S. Ostapchenko, Phys. Rev. D **83**, 014018 (2011); Eur. Phys. J. Web Conf. **52**, 02001 (2013).
[5] T. Pierog et al., arXiv:1306.0121.
[6] E.-J. Ahn et al., in Proceedings of the 33rd Int. Cosmic Ray Conf., Rio de Janeiro, 2013.
[7] T. Pierog, Eur. Phys. J. Web Conf. **53**, 01004 (2013).
[8] G. Farrar (Pierre Auger Collaboration), in Proceedings of the 33rd Int. Cosmic Ray Conf., Rio de Janeiro, 2013.
[9] W. D. Apel et al. (KASCADE-Grande Collaboration) (to be published).
[10] G. Antchev et al. (TOTEM Collaboration), Europhys. Lett. **96**, 21002 (2011).
[11] G. Antchev et al. (TOTEM Collaboration), Europhys. Lett. **101**, 21002 (2013).
[12] G. Antchev et al. (TOTEM Collaboration), Europhys. Lett. **101**, 21003 (2013).
[13] G. Antchev et al. (TOTEM Collaboration), Europhys. Lett. **101**, 21004 (2013).
[14] G. Antchev et al. (TOTEM Collaboration), Phys. Rev. Lett. **111**, 012001 (2013).
[15] R. J. Glauber, in Lectures in Theoretical Physics: Lectures Delivered at the Summer Institute for Theoretical Physics, University of Colorado, Boulder, edited by W. E. Britten (Interscience, New York, 1959), Vol. 1, p. 315.
[16] V. N. Gribov, Sov. Phys. JETP **29**, 483 (1969).
[17] R. D. Parsons, C. Bleve, S. S. Ostapchenko, and J. Knapp, Astropart. Phys. **34**, 832 (2011).
[18] B. Abelev et al. (ALICE Collaboration), Eur. Phys. J. C **73**, 2456 (2013).
[19] G. Aad et al. (ATLAS Collaboration), Eur. Phys. J. C **72**, 1926 (2012).
[20] CMS Collaboration, Report No. CMS-PAS-FSQ-12-005.
[21] G. Antchev et al. (TOTEM Collaboration), Phys. Rev. Lett. **111**, 262001 (2013).
[22] F. Oljemark (TOTEM Collaboration), in 15th Int. Conf. on Elastic and Diffractive Scattering, Saariselkä, 2013.
[23] V. A. Khoze, A. D. Martin, and M. G. Ryskin, Eur. Phys. J. C **74**, 2756 (2014).
[24] V. A. Khoze, A. D. Martin, and M. G. Ryskin, arXiv:1402.2778.

[25] S. Ostapchenko, Phys. Lett. B **703**, 588 (2011).

[26] S. Ostapchenko, Phys. Rev. D **81**, 114028 (2010).

[27] K. Nakamura *et al.* (Particle Data Group), J. Phys. G **37**, 075021 (2010).

[28] G. Aad *et al.* (ATLAS Collaboration), New J. Phys. **13**, 053033 (2011).

[29] CMS Collaboration, Report No. CMS-PAS-QCD-10-024.

[30] T. Bergmann, R. Engel, D. Heck, N. Kalmykov, S. Ostapchenko, T. Pierog, T. Thouw and K. Werner, Astropart. Phys. **26**, 420 (2007).

[31] H. Sagawa, in *33rd Int. Cosmic Ray Conf., Rio de Janeiro, 2013*.

[32] R. Aloisio, V. Berezinsky, P. Blasi, and S. Ostapchenko, Phys. Rev. D **77**, 025007 (2008).

[33] R. Aloisio, V. Berezinsky, and A. Gazizov, Astropart. Phys. **39**–**40**, 129 (2012).

[34] R. Ulrich, R. Engel, and M. Unger, Phys. Rev. D **83**, 054026 (2011).

[35] S. Ostapchenko, Nucl. Phys. B, Proc. Suppl. **151**, 143 (2006); AIP Conf. Proc. **928**, 118 (2007).